Available online at www.sciencedirect.com

ScienceDirect

Advances in Space Research 55 (2015) 2248–2255

ADVANCES IN SPACE RESEARCH (a COSPAR publication)

www.elsevier.com/locate/asr

Research on global plasmaspheric electron content by using LEO occultation and GPS data

Peng Chen [a,b,*], Yibin Yao [c,d]

[a] College of Geomatics, Xi'an University of Science and Technology, Xi'an 710054, China
[b] State Key Laboratory of Geodesy and Earth's Dynamics, Wuhan 430077, China
[c] School of Geodesy and Geomatics, Wuhan University, Wuhan 430079, China
[d] Key Laboratory of Geospace Environment and Geodesy, Ministry of Education, Wuhan University, Wuhan 430079, China

Received 26 February 2014; received in revised form 1 February 2015; accepted 3 February 2015
Available online 11 February 2015

Abstract

This paper investigates the characteristics of global plasmaspheric electron content (pTEC) using COSMIC (Constellation Observing System for Meteorology, Ionosphere and Climate) occultation and GPS (Global Positioning System) data. The ionospheric electron content (iTEC) within 100–1000 km was obtained by fitting the COSMIC occultation electron density profiles, and the pTEC was obtained by subtracting the iTEC from CODE (Center for Orbit Determination in Europe) GIM (global ionosphere maps) TEC provided by University of Bern. This paper also investigates the characteristics of pTEC variations with local time, latitude and season. The results show that in 2011, the worldwide average of pTEC was 4.02 TECu, which is consistent with the findings of other studies. The pTEC shows significant diurnal variation characteristics, that is, pTEC is higher during daytime than during nighttime, but the percentage contribution of pTEC to GPS TEC is higher during nighttime than during daytime. The pTEC varies with the seasons, pTEC hemispheres symmetrically during spring and autumn, while pTEC in the summer hemisphere is higher than that in the winter hemisphere. Moreover, the percentage contribution of pTEC to GPS TEC (total electron content) is higher in winter hemisphere than in summer hemisphere.

Keywords: Plasmasphere; Ionosphere; Electronic content; COSMIC; GPS

1. Introduction

Plasmasphere is a part of the Earth's magnetic layer, contains low energy plasma, located above the ionosphere, and has height that can be extended 3–5 times the Earth's radius. The plasmasphere has electron density that is over several orders smaller than the ionosphere (Gallagher et al., 2000), but it has a large height, and thus, in some cases (such as at night and under the solar quiet period) the contribution of plasmaspheric electron content cannot be ignored (Cherniak et al., 2012).

GPS is currently widely used in ionospheric research. TEC is one of the most important parameters used in the ionospheric studies. The dense network of the GPS receivers allows the simultaneous coverage of TEC values in global scale with high temporal resolution (Jee et al., 2010; Klimenko et al., 2014). The total electron content along the GPS signal propagation path is called the GPS TEC, the value of which can be seen as the sum of the ionospheric electron content (iTEC) and the plasmasphere electron content (pTEC).

Traditional methods used for obtaining iTEC are mainly divided into two categories as follows: the use of the empirical model of the ionosphere and the use of ionosonde or other means of ground observations (Huang and Reinisch, 2001; Reinisch and Huang, 2001). Guiter et al.

* Corresponding author at: College of Geomatics, Xi'an University of Science and Technology, Xi'an 710054, China.
E-mail address: chenpeng0123@gmail.com (P. Chen).

http://dx.doi.org/10.1016/j.asr.2015.02.004
0273-1177/

(1995) modeled the plasmaspheric density using a time-dependent model and found the annual variation of plasmaspheric electron density is related to the annual variations in the upper ionospheric O+ density. Richards et al. (2000) examined the relative importance of ionospheric and thermospheric densities and temperatures in producing the annual variation in the plasmaspheric electron density. Lunt et al. (1999a) and Balan et al. (2002) used the SUPIM (Sheffield University Plasmasphere Ionosphere Model) model to obtain the pTEC, and then they explored the various characteristics of pTEC to obtain an initial understanding of pTEC. Webb and Essex (2004) created the three-dimensional Global Plasmasphere Ionosphere Density (GPID) model simulates the global-scale dynamics of the ion and electron densities within the plasmasphere. Belehaki et al. (2004) and Mosert et al. (2007) investigated the various characteristics of the pTEC at Athens and Ebro by using GPS TEC and ionosonde data and were able to obtain more consistent results. However, the ionosonde is only distributed in a limited number of land areas and it can only detect the ionosphere under the F2 peak height. The electron density profile above the F2 peak height can only be obtained via fitting, and thus, accurate research on the global plasmaspheric electron content cannot be obtained. Yizengaw et al. (2008) estimated the relative contribution of the plasmaspheric electron content to the ground-based GPS TEC using ground-based GPS TEC and JASON-1 TEC. The results showed the relative contribution of the plasmaspheric electron content exhibits a diurnal variation and the contribution is also maximum at the equatorial region. Lee et al. (2013) compared the global pTEC with the ionospheric TEC simultaneously measured by Jason-1 satellite during the declining phase of solar cycle 23, their study showed that the plasmaspheric density structures fundamentally follow the ionosphere, but there are also significant differences between them. Chong et al. (2013) used the Millstone Hill incoherent scatter radar (ISR) observations to investigate Millstone Hill area's pTEC characteristics. The advantage of ISR is that it is possible to construct the vertical profile of the electron density above the F2 layer peak height, but it can only get localized plasmaspheric electronic content characteristics.

The current paper presents a method that makes use of the COSMIC occultation and ground-based GPS data to investigate the worldwide pTEC characteristics. Moreover, the characteristics of pTEC variation are analyzed using several geographical parameters, such as local time, season, latitude, solar radiation, and geomagnetic activity. The COSMIC occultation data have good global distribution characteristics, and the ionospheric electron content obtained has high accuracy (Tsai et al. 2001, 2009; Jakowski et al., 2005). Both the COSMIC occultation and ground-based GPS data can be used to investigate pTEC, consequently surpassing existing research methods that only investigate localized effects. Ground-based GPS observations data were used to obtain global GPS TEC, and COSMIC occultation data were used to obtain ionospheric total electron content iTEC under 1000 km. The difference between them can be seen as pTEC.

2. Data and data processing

2.1. CODE global ionospheric maps

Global GPS tracking station provides an approach for accessing global high-resolution GPS TEC. In 1998, IGS began providing global ionosphere products in resolutions of 5° longitude and 2.5° latitude at a temporal resolution of 2 h. Currently, four data processing centers, namely, CODE, JPL, ESA and UPC, provide global ionosphere products, while various analysis centers use different ground tracking station observation data and different methods to establish a global ionospheric model. With the increase in the number of GPS ground tracking stations and the refinement of the data processing method, the accuracy of IGS ionospheric products increases, making it an indispensable resource for studies on the variations of the global ionosphere.

CODE is one of the first agencies in the world that investigated ionospheric modeling and is also currently the only data analysis center that uses GPS and GLONASS (Global Navigation Satellite System) for ionospheric modeling. CODE provides global ionospheric final products by using more than 200 worldwide GPS/GLONASS tracking stations observation data and a 15×15 order spherical harmonic function model with spatial resolutions of $5^\circ \times 2.5^\circ$ at a temporal resolution of 2 h. In this paper, GPS TEC from the bottom ionosphere to 20,200 km is obtained using CODE's global ionospheric grid data.

The error source of GIM include: spherical symmetry assumption when converting slant TEC to vertical TEC, differential code bias estimation, pseudo range noise and some other errors. Thus, the value of GIM's error is about several TECu.

2.2. COSMIC occultation ionospheric data

LEO occultation can be used to obtain the ionospheric vertical profile under LEO satellite orbits (Jakowski et al., 2005; Liou et al., 2007). The COSMIC satellite system developed jointly by the United States and Chinese Taiwan is currently the most commonly used LEO occultation system, and its number of occultation events and data accuracy are significantly better compared with those in previous occultation systems. The COSMIC system, which was launched on April 15, 2006, consists of six small satellites with an orbital height of 700–800 km and an orbital inclination of 72°. Satellite on board GPS occultation devices can achieve troposphere and ionosphere occultation. Such system can obtain 1500–2500 globally distributed effective occultation observations daily, 70% of which can obtain final electron density.

The COSMIC radio occultation electron density profile is retrieved based on several assumptions with spherical

symmetry assumption the most significant error source. The Abel inversion could have significant error in equatorial and lower latitude and lower altitude region.

In this paper, COSMIC level 2 products "ionprf" provide the ionospheric electron content iTEC that is obtained using the electron density profile data for 100–700 km during an occultation event. Data processing is divided into three parts, namely, profile fitting, data filtering, and integral calculation. The chapman-α function of varying scale height used for electron density profile fitting can be written as follows (Fox, 1994; Chong et al., 2013):

$$N_e(h) = N_mF_2 \exp[0.5(1 - z - e^{-z})]$$
$$z = (h - h_mF_2)/H(h) \quad (1)$$

where, N_mF_2 and h_mF_2 is the ionospheric F2 layer peak electron density and peak height, respectively. The chapman-α function of varying scale height can better reflect the electron density at different height variations with height (Fox, 1994). The scale height under the peak height is $H(h) = A_1(h - h_mF_2) + H_m$, and the scale height above the peak height is $H(h) = A_2(h - h_mF_2) + H_m$, and the unknown parameters N_mF_2, h_mF_2, A_1, A_2 and H_m can be obtained using the method of non-linear least squares.

Fig. 1 shows the COSMIC occultation electron density fitting results that were obtained using chapman-α function of varying scale height. The fitting results and the occultation observations yielded excellent degree of compliance. During data processing, a small portion of the profiles whose deviation exceeded the tolerance were removed to ensure the high reliability of the fitting electron density results at 100–1000 km. The method mentioned above was used to obtain fitting profiles, which were then integrated to obtain the total electron content within 100–1000 km at the position of maximum electron density of each occultation event.

3. Comparison of GPS TEC and COSMIC TEC

Fig. 2 shows the scatter map of GPS TEC and COSMIC TEC, where COSMIC TEC is the abscissa, GPS TEC is the vertical coordinate, and the straight line is the least-squares

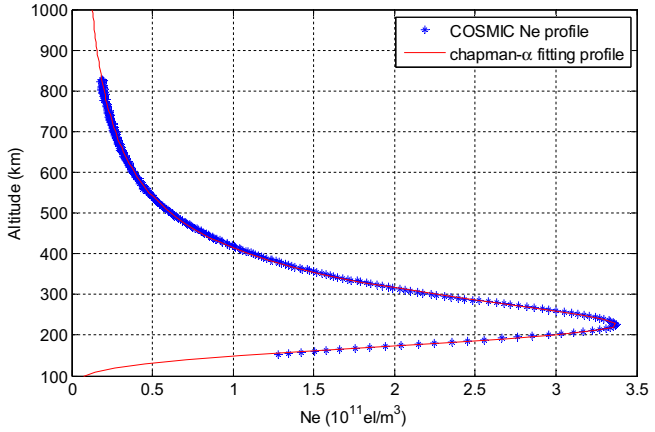

Fig. 1. Occultation electron density fitting results obtained using the chapman-α function.

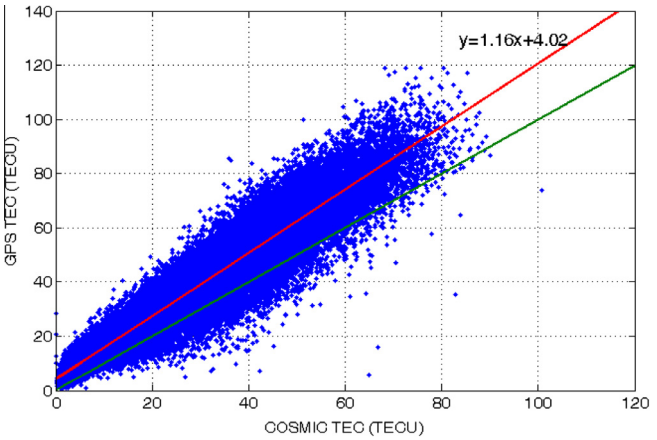

Fig. 2. Scatter plot of COSMIC TEC and GPS TEC (the red straight line denotes the least-squares fitting results). (For interpretation of the references to color in this figure legend, the reader is referred to the web version of this article.)

fitting of the two results. As can be seen in the figure, the GPS TEC and COSMIC TEC have good correlation. According to the linear regression equation, the GPS TEC and COSMIC TEC have a difference of 4.02 TECu, indicating that the global average magnitude of pTEC was 4.02 TECu in 2011. Lunt et al. (1999) used GPS and NIMS (Navy Ionospheric Monitoring System) data to investigate the variation character of the plasmasphere at high latitudes in Europe and found pTEC to decrease with increasing latitude at approximately 2 TECu at 50.4°N. Belehaki et al. (2004) used the GPS TEC and ionosonde TEC to investigate the plasmaspheric electron content at Athens station, and their results show that the two had a difference of approximately 6.3 TECu between October 2000 and September 2001. Breed et al. (1997) found a plasmaspheric electron content of approximately 7.2 TECu at Australia Salisbury Station (34.8°S) in December 1992. Chong et al. (2013) used the Millstone Hill ISR data and obtained Millstone Hill station area plasmaspheric electron content of approximately 5.6 TECu. Thus, even though various studies used different observation techniques, research time and location, they obtained plasmaspheric electron content with roughly the same order of magnitude, indicating the reliability of the plasmaspheric electron content obtained in the current paper by using GPS and COSMIC. However, since the error of observation is inevitable, part of COSMIC TEC equal to or even greater than GPS TEC (point located at and below the green line in Fig. 2), leads pTEC equal to zero or even less than zero, this is nonexistent in reality, and thus we remove those pTEC less than or equal to zero in subsequent studies.

4. The variation characteristics of pTEC

4.1. The global distribution characteristics of pTEC

Fig. 3 shows the pTEC variation with local time and latitude in March, June, September and December 2011,

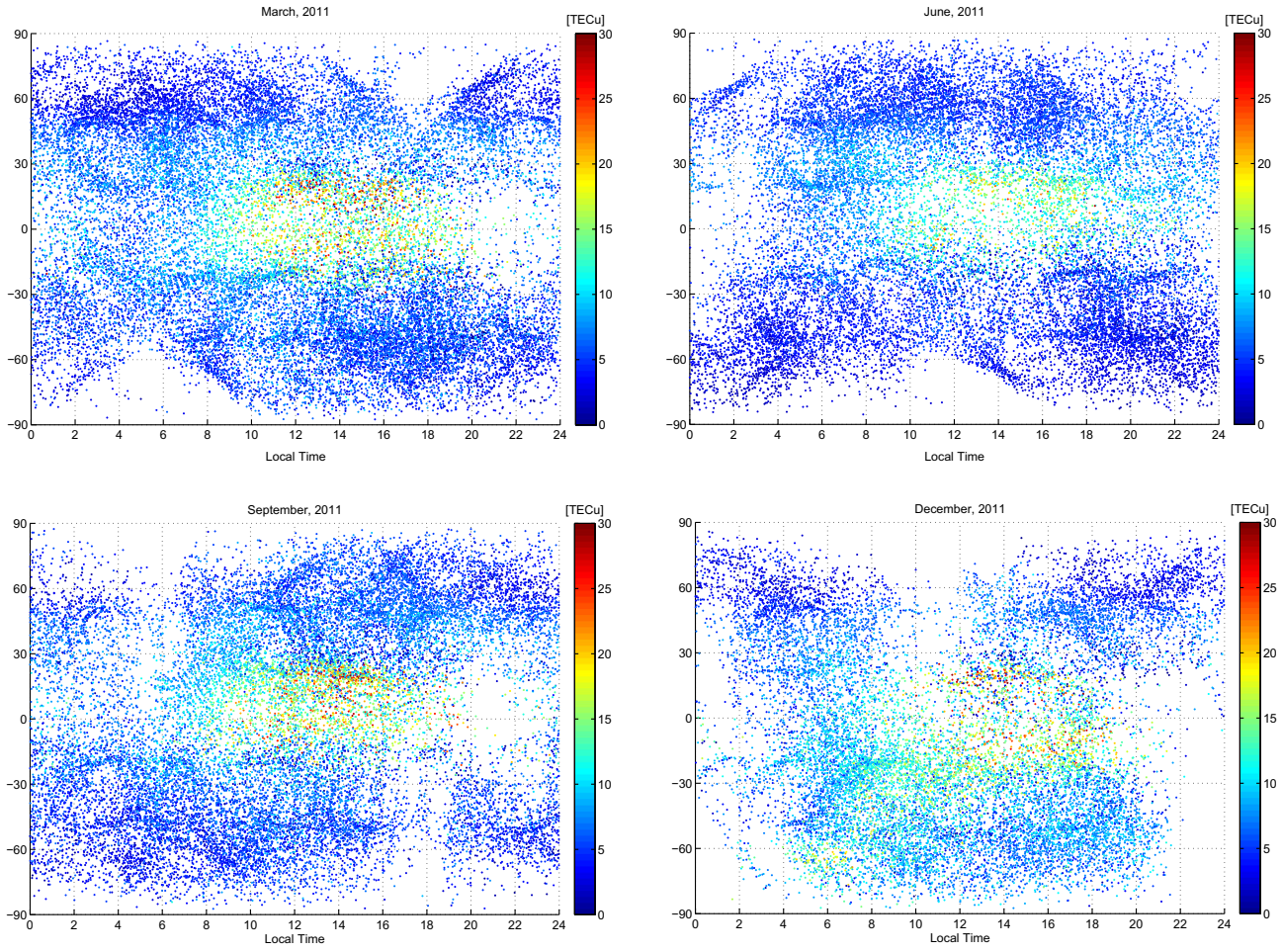

Fig. 3. The plasmaspheric electron content pTEC variation with local time and latitude in March, June, September, and December 2011.

respectively. As can be seen in this figure, pTEC had significant correlations with local time and latitude. The pTEC peak occurred at LT 12:00–16:00 in all seasons, with the minimum occurring during nighttime. The maximum value was initially near the equator and then gradually decreased from the equator to the direction of the poles. Unlike the ionospheric electron content, no apparent equatorial anomaly phenomenon was observed. In addition, the results show the different distribution characteristics of pTEC in different seasons. InMarch and September, the pTEC was uniformly distributed in the northern and southern hemispheres, and in June and December, it was higher in the summer hemisphere than in the winter hemisphere. These results are consistent with the distribution characteristics of the ionospheric electron content.

Fig. 4 shows the percentage contribution of pTEC to GPS TEC variation with local time and latitude. As can be seen in the figure, the percentage contribution of pTEC reached maximum during nighttime, lower during daytime, and opposite to the diurnal variation characteristics of pTEC. In addition, the percentage contribution of pTEC shared obvious seasonal characteristics; the percentage contributions of pTEC at different latitudes were not significantly different at the same local time in March and September. But in June and December, the percentage contribution exhibited completely opposite characteristics, wherein it was significantly higher in the summer hemisphere than in the winter hemisphere and was higher in high latitudes than in low latitudes.

4.2. Diurnal variation

Fig. 5 shows the plasmaspheric electron content pTEC and the percentage contribution of pTEC to GPS TEC variation with local time in 2011. As can be seen in the figure, the pTEC and the percentage contribution of pTEC to GPS TEC exhibited obvious diurnal variation characteristics. The pTEC was significantly higher during daytime than during nighttime. Moreover, it reached the maximum of approximately 7.8 TECu at LT 12:00–14:00 gradually decreased to theminimum at LT 22:00 of∼5 TECu, and then gradually increased. The percentage contribution of pTEC to GPS TEC was significantly higher during nighttime than during daytime. Moreover, it reached the maximum of 55% at LT 04:00, but was only 25% at LT 12:00–14:00.

The diurnal variation of the ionosphere is mainly driven by solar energy. The ionospheric electron density reaches

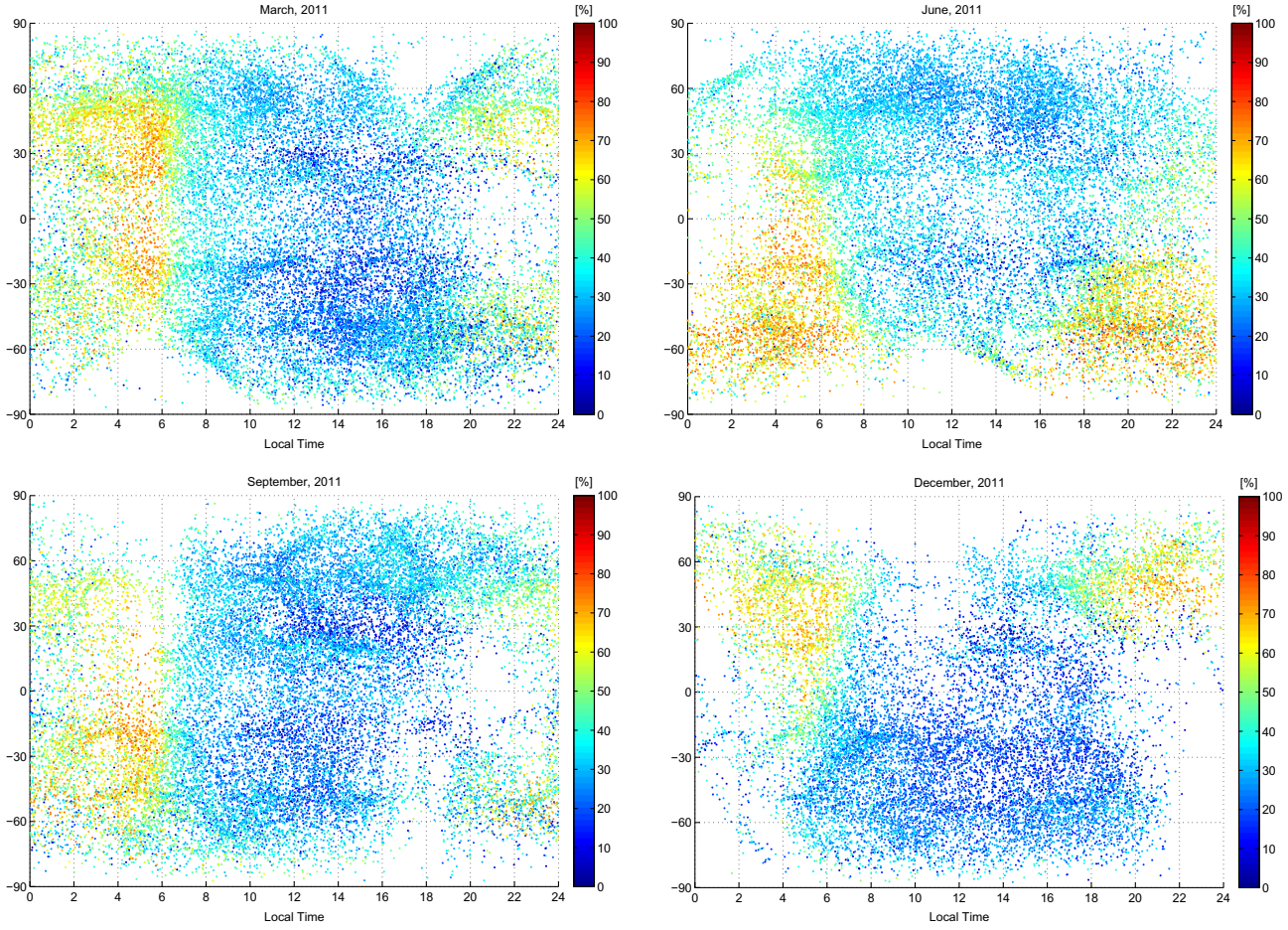

Fig. 4. The percentage contribution of pTEC to GPS TEC variation with local time and latitude in March, June, September and December, 2011.

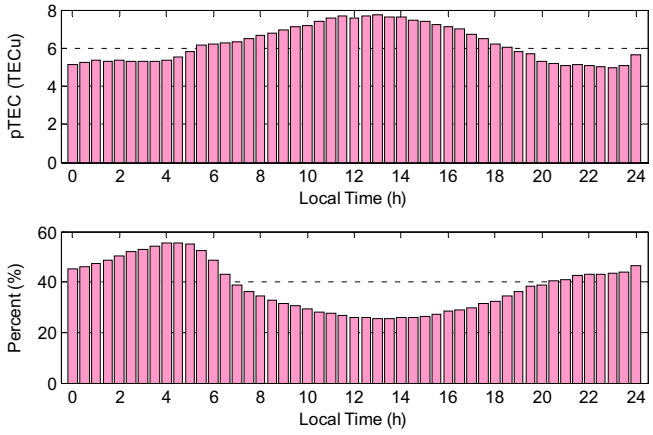

Fig. 5. The pTEC and the percentage contribution of pTEC to GPS TEC variation with local time in 2011.

its maximum value at noon, while the diurnal variation of the plasmaspheric is mainly related to the coupling to the ionosphere. During daytime, the ionosphere electron diffuse up into the plasmasphere, the electron content in the plasmasphere increases, and the plasmaspheric electron content decreases mainly because of the electron diffusion back to the ionosphere at night. During daytime with solar radiation increasing, the ionospheric electron content increased rapidly, reducing the percentage contribution of pTEC to GPS TEC. On the other hand, during nighttime, solar radiation weakened rapidly, ions and free electrons recombined, the ionospheric electron content decreased sharply, and the percentage contribution of pTEC to GPS TEC increased.

4.3. Annual variation

Fig. 6 shows the pTEC and the percentage contribution of pTEC to GPS TEC variation with months in the northern and southern hemispheres, respectively. In fact, COSMIC TEC can be obtained for all longitudes in contrast to GPS TEC that have good coverage in the Northern Hemisphere and only two regions (South America and Australia) in Southern Hemisphere.

As can be seen in the figure, the annual variation of pTEC and the percentage contribution of pTEC to GPS TEC exhibited significant differences in the northern and southern hemispheres. The pTEC in the northern hemisphere reached maximum in October and minimum in January. With regard to season, the pTEC was higher in equinox but lowest in winter. The pTEC in the southern hemisphere reached maximum in December and minimum

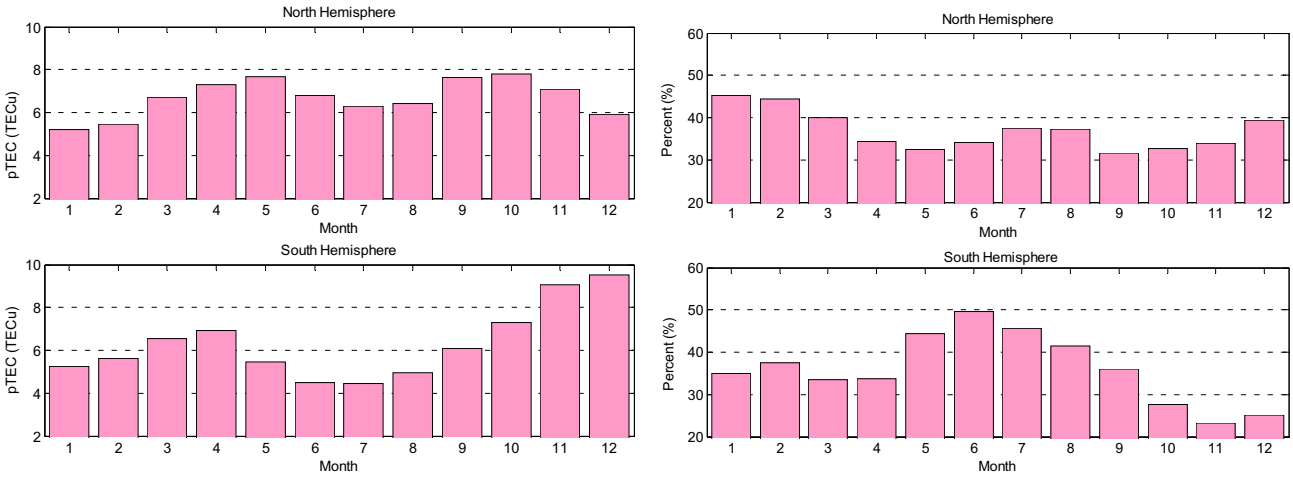

Fig. 6. The pTEC and the percentage contribution of pTEC to GPS TEC variation with months in the northern and southern hemispheres.

in July. With regard to season, the pTEC was highest in autumn and lowest in summer.

The percentage contribution of pTEC to GPS TEC also exhibited variations in different hemispheres. In the northern hemisphere, the lowest value was obtained in September and the highest in January; the lower in spring and autumn and the highest in winter. In the southern hemisphere, the highest value was obtained in June and the lowest in November; the highest in summer and the lowest in autumn. These results also indicate that the characteristics of pTEC variation were opposite to the percentage contribution of pTEC to GPS TEC. The percentage contribution of pTEC to GPS TEC was smaller with larger pTEC, which is consistent with the conclusions of other studies that used different methods.

The results show that the pTEC variation is consistent with the ionospheric electron content, that is, it is minimum in the winter hemisphere and higher in solstice than in equinox. The seasonal variations of ionospheric electron content are mainly caused by seasonal changes in neutral components and the dynamics of the ionosphere (Richards, 2001; Jee et al., 2004), while the plasmasphere only contains small amounts of ion and neutral components. Therefore, during the quiet period, the seasonal variations of pTEC are mainly caused by the seasonal changes in plasmasphere–ionosphere coupling. In addition, in the Southern Hemisphere the diurnal variation in pTEC includes some longitudinal dependence due to the different special data coverage of COSMIC TEC and GPS TEC.

4.4. Variations with latitude

Taking 5° in latitude direction as an interval, the pTEC and the percentage contribution of pTEC to GPS TEC variation with latitude were analyzed according to different seasons and during daytime (LT 08:00–20:00) and nighttime (LT 20:00–08:00).

Fig. 7(a) shows the pTEC of different seasons varying with latitude during daytime, wherein the pTEC was generally higher at low latitudes than at high latitudes in different seasons and no apparent equatorial anomaly was observed. The variation characteristics in March and September were consistent, the pTEC maximum value was near the equator and higher than the two other months. In June, pTEC maximum was moved to 15°N in the northern hemisphere and only reached a maximum of 12 TECu, which is the lowest value in four months. In December, the pTEC maximum at 10°S in the southern hemisphere. In addition, in March, September and December, the pTEC exhibited a significant trough phenomenon near 20–40°N, the reason for which requires further analysis.

Fig. 7(b) shows the pTEC of different season variation with latitude during nighttime. As can be seen in the figure, the pTEC between 30°S and 30°N was significantly lower during nighttime than during daytime, but only slightly changed in other regions. In addition, no apparent trough phenomenon between 20°N and 40°N was observed, but the pTEC of this region was higher during nighttime than during daytime. The variations were roughly the same in all months except December, both reached the maximum in the equatorial region. In December, the southern hemisphere pTEC was significantly higher than in the other three months.

Fig. 8(a) shows the percentage contribution of pTEC to GPS TEC variation with different latitudes during daytime. In March and September, the variation regularity was consistent; higher in high latitudes than in low latitudes, had an average of ~30%, and the obvious trough phenomenon occurred in the vicinity of 30°N and 25°S. In June, the percentage contribution of pTEC to GPS TEC was higher in the area south of 30°N than in the other three months, especially in the area south of 15°S, had a maximum of 55%, and was higher than in the other three months by ~20%. In December, the percentage contribution of pTEC to GPS TEC was lower than in the other three months in the area south of 30°N and higher than in the other three months in the area north of 40°N.

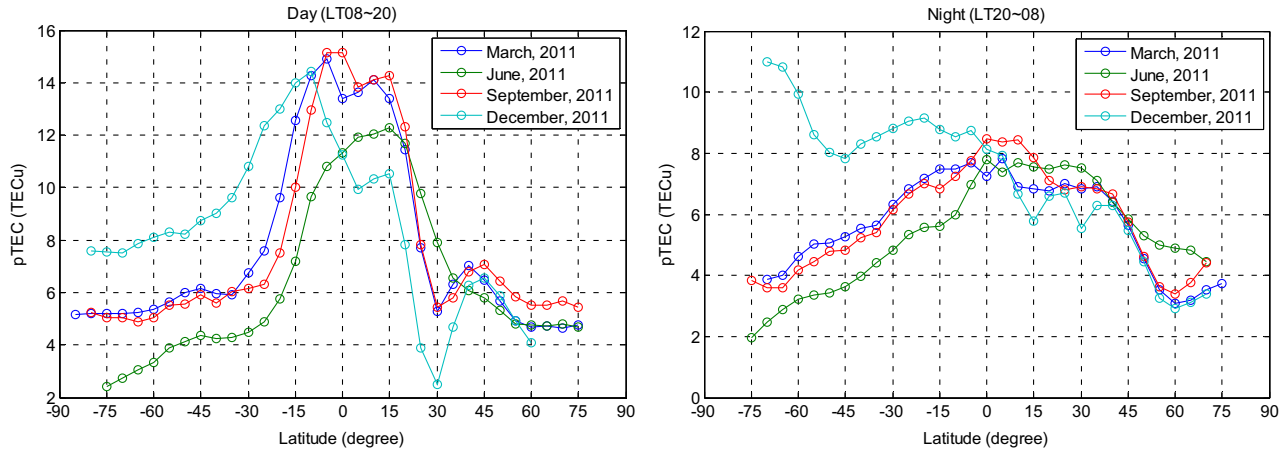

Fig. 7. The pTEC versus latitude in different seasons (a) during daytime and (b) during nighttime.

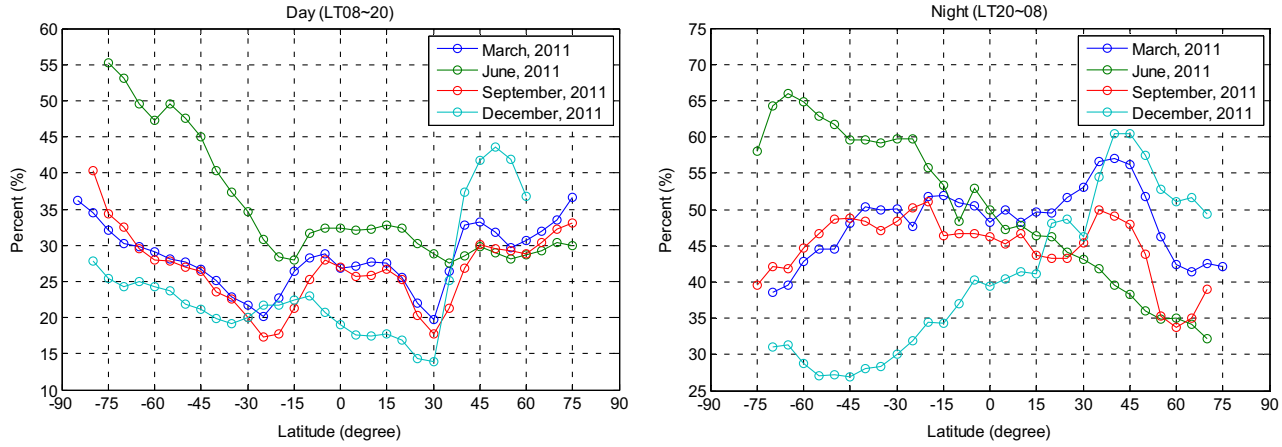

Fig. 8. The percentage contribution of pTEC to GPS TEC versus latitude in different seasons (a) during daytime and (b) during nighttime.

Fig. 8(b) shows the percentage contribution of pTEC to GPS TEC variation with different latitudes during nighttime. The percentage contribution was significantly higher during nighttime than during daytime with an average of ~50%. In March and September, no significant difference was observed in the area south of 15°N, while the percentage contribution in the area north of 15°N in March was 5% higher than in September. In June, the percentage decreased from south to north by over 65% at 65°S but only 32% at 70°N. In December and June, the overall varies in the contrary, the percentage increased gradually from south to north by over 60% at 45°N but only 32% at 65°S. In addition, the percentage exhibited significant peak phenomenon at 35–45°N in all months except in June.

5. Conclusions

This paper presented a method of research on plasmaspheric electron content by using COSMIC occultation and ground-based GPS data. Moreover, this paper analyzed the characteristics of pTEC variation with several geophysical parameters, such as local time, latitude and season.

Given that the ions and free electrons in the plasmasphere mainly come from the ionospheric ions and free electrons spread upward, the variation of the plasmasphere is mainly driven by the ionosphere–plasmasphere coupling, thereby showing some similar properties with the ionosphere. The results show that pTEC exhibited significant diurnal variation characteristics, that is, pTEC was higher during daytime than during nighttime, but the percentage contribution of pTEC to GPS TEC was higher during nighttime than during daytime. Overall, the pTEC decreased from the equator to the two poles. Moreover, the pTEC varied with the seasons; it hemispheres symmetrical in spring and autumn, and it is higher in the summer hemisphere than in the winter hemisphere. However, the percentage contribution of pTEC to GPS TEC was higher in the winter hemisphere than in the summer hemisphere and was higher at high latitudes than at low latitudes.

Further investigations will make use of more data on the characteristics of pTEC variation and include ocean altimetry satellite and other type's observations to improve reliability.

Acknowledgments

GIM-TEC maps are provided by University of Bern, at ftp.unibe.ch/aiub/CODE/. Thanks CDAAC provide COSMIC "ionprf" data. This research was supported by the National Natural Science Foundation of China (41404031), State Key Laboratory of Geodesy and Earth's Dynamics Fund (SKLGED2013-4-10-EB), State Key Laboratory of Information Engineering in Surveying Mapping and Remote Sensing Fund (13S03), Key Laboratory of Geo-informatics of State Bureau of Surveying and Mapping Fund (201318, 201420), the Surveying and Mapping Foundation Research Fund Program, State Bureau of Surveying and Mapping (12-01-07).

References

Balan, N., Otsuka, Y., Tsugawa, T., et al., 2002. Plasmaspheric electron content in the GPS ray paths over Japan under magnetically quiet conditions at high solar activity. Earth, Planets Space 54 (1), 71–79.

Belehaki, A., Jakowski, N., Reinisch, B.W., 2004. Plasmaspheric electron content derived from GPS TEC and digisonde ionograms. Adv. Space Res. 33 (6), 833–837.

Breed, A.M., Goodwin, G.L., Vandenberg, A.M., Essex, E.A., Lynn, K.J.W., Silby, J.H., 1997. Ionospheric total electron content and slab thickness determined in Australia. Radio Sci. 32 (4), 1635–1643.

Cherniak, Iu.V., Zakharenkova, I.E., Krankowski, A., Shagimuratov, I.I., 2012. Plasmaspheric electron content derived from GPS TEC and FORMOSAT-3/COSMIC measurements: solar minimum condition. Adv. Space Res. 50, 427–440.

Chong, XiaoYan, Zhang, ManLian, Zhang, ShunRong, et al., 2013. An investigation on plasmaspheric electron content derived from ISR and GPS observations at Millstone Hill. Chin. J. Geophys. 56 (3), 738–745.

Fox, M.W., 1994. A simple, convenient formalism for electron density profiles. Radio Sci. 29 (6), 1473–1491.

Gallagher, D.L., Craven, P.D., Comfort, R.H., 2000. Global core plasma model. J. Geophys. Res.: Space Phys. (1978–2012) 105 (A8), 18819–18833.

Guiter, S.M., Rasmussen, C.E., Gombosi, T.I., et al., 1995. What is the source of observed annual variations in plasmaspheric density? J. Geophys. Res. 100 (A5), 8013–8020.

Huang, X., Reinisch, B.W., 2001. Vertical electron content from ionograms in real time. Radio Sci. 36 (2), 335–342.

Jakowski, N., Tsybulyal, K., Stankov, S.M., et al., 2005. About the potential of GPS radio occultation measurements for exploring the ionosphere. In: Earth observation with CHAMP. Springer, Berlin Heidelberg, pp. 441–446.

Jee, G., Schunk, R.W., Scherliess, L., 2004. Analysis of TEC data from the TOPEX/poseidon mission. J. Geophys. Res.: Space Phys. (1978–2012) 109 (A1).

Jee, G., Lee, H.B., Kim, Y.H., et al., 2010. Assessment of GPS global ionosphere maps (GIM) by comparison between CODE GIM and TOPEX/Jason TEC data: ionospheric perspective. J. Geophys. Res. 115 (A10), A10319.

Klimenko, M.V. et al., 2014. The global morphology of the plasmaspheric electron content during Northern winter 2009 based on GPS/COSMIC observation and GSM TIP model results. Adv. Space Res.

Lee, H.B., Jee, G., Kim, Y.H., et al., 2013. Characteristics of global plasmaspheric TEC in comparison with the ionosphere simultaneously observed by Jason-1 satellite. J. Geophys. Res.: Space Phys.

Liou, Y.A., Pavelyev, A.G., Liu, S.F., et al., 2007. FORMOSAT-3/COSMIC GPS radio occultation mission: preliminary results. IEEE Trans. Geosci. Remote Sens. 45 (11), 3813–3826.

Lunt, N., Kersley, L., Bailey, G.J., 1999a. The influence of the protonosphere on GPS observations: model simulations. Radio Sci. 34 (3), 725–732.

Lunt, N., Kersley, L., Bishop, G.J., et al., 1999b. The contribution of the protonosphere to GPS total electron content: experimental measurements. Radio Sci. 34 (5), 1273–1280.

Mosert, M., Gende, M., Brunini, C., et al., 2007. Comparisons of IRI TEC predictions with GPS and digisonde measurements at Ebro. Adv. Space Res. 39 (5), 841–847.

Reinisch, B.W., Huang, X., 2001. Deducing topside profiles and total electron content from bottomside ionograms. Adv. Space Res. 27 (1), 23–30.

Richards, P.G., 2001. Seasonal and solar cycle variations of the ionospheric peak electron density: comparison of measurement and models. J. Geophys. Res.: Space Phys. (1978–2012) 106 (A7), 12803–12819.

Richards, P.G., Chang, T., Comfort, R.H., 2000. On the causes of the annual variation in the plasmaspheric electron density. J. Atmos. Solar Terr. Phys. 62 (10), 935–946.

Tsai, L.C., Tsai, W.H., Schreiner, W.S., et al., 2001. Comparisons of GPS/MET retrieved ionospheric electron density and ground based ionosonde data. Earth, Planets Space 53 (3), 193–205.

Tsai, L.C., Liu, C.H., Hsiao, T.Y., 2009. Profiling of ionospheric electron density based on FormoSat-3/COSMIC data: results from the intense observation period experiment. Terr. Atmos. Oceanic Sci. 20 (1), 181.

Webb, P.A., Essex, E.A., 2004. A dynamic global model of the plasmasphere. J. Atmos. Solar Terr. Phys. 66 (12), 1057–1073.

Yizengaw, E., Moldwin, M.B., Galvan, D., et al., 2008. Global plasmaspheric TEC and its relative contribution to GPS TEC. J. Atmos. Solar Terr. Phys. 70 (11), 1541–1548.

Further reading

Mazzella, A.J., 2009. Plasmasphere effects for GPS TEC measurements in North America. Radio Sci. 44 (5).